Geostatistical Model for Forecasting Spatial Dynamics of Defoliation Caused by the Gypsy Moth (Lepidoptera: Lymantriidae)

MICHAEL E. HOHN,[1] ANDREW M. LIEBHOLD,[2] AND LINDA S. GRIBKO[1]

Environ. Entomol. 22(5): 1066–1075 (1993)

ABSTRACT Outbreaks of the gypsy moth, *Lymantria dispar* (L.), typically occur over large areas but are difficult to predict. Previously developed models forecast defoliation from preseason counts of egg masses in a given stand. In this study, we take a different approach to defoliation prediction: forecasts are based upon the statistical autocorrelation of defoliation through space and time. Spatial and temporal autocorrelation of defoliation in historical data was quantified at a variety of scales using variograms. We used a 30-yr time series of aerial sketch maps of gypsy moth defoliation in Massachusetts to calculate these variograms. The variograms were then used to parameterize a geostatistical estimation technique: three-dimensional simple kriging. Kriged estimates are weighed averages of values from nearby locations and are typically used to interpolate two-dimensional data. In this study, we used kriging to extrapolate future defoliation maps into a third dimension, time. Kriged estimates were expressed as probabilities of detectable defoliation. Predicted probabilities were estimated for each year of the time series and were compared with actual defoliation maps for that year. The kriging procedure usually performed well in predicting the spatial distribution of outbreaks in a given year, but the magnitude of regionwide outbreaks generally lagged a year behind actual values. Though this approach is not currently suitable for operational use, it represents a novel approach to landscape-level forecasting of insect outbreaks, These models may ultimately outperform current forecasting systems.

KEY WORDS *Lymantria dispar*, kriging, variogram

THE GYPSY MOTH, *Lymantria dispar* (L.), is an example of an eruptive species (Price et al. 1990). Population densities vary through several orders of magnitude, often reaching epidemic densities that have spectacular effects on their habitat (i.e., total defoliation of host trees). It is not uncommon for gypsy moth populations to persist for many years at densities that are so low that it may be difficult to detect any life stages except male moths. Occasionally, for unknown reasons, population densities increase, often to defoliating levels of >6,000 egg masses per ha, within only a few generations. These outbreak populations may persist for several years before collapsing.

Gypsy moth outbreaks often occur over very large areas but are notoriously difficult to predict (Liebhold & Elkinton 1989). Previous models developed for predicting defoliation have been based mostly upon preseason counts of egg masses (Gansner & Herrick 1982, Montgomery 1990, Williams et al. 1991, Liebhold et al. 1993a). Though there is a significant relationship between egg mass density and subsequent defoliation at the stand level, the variance about this relationship is great. Consequently, considerable error is encountered in using this method for prediction of defoliation. The lack of a more precise method for prediction of defoliation can have a devastating effect on the efficiency of the gypsy moth management program (Ravlin et al. 1987).

Previous models developed for predicting outbreaks have relied on data collected at a single point and have mostly ignored spatial processes. Twenty-five years ago, Campbell (1967) recognized that the dynamics of gypsy moth populations are affected by population densities in nearby areas; populations are often sychronized in their yearly fluctuations during the development of gypsy moth outbreaks (Liebhold & McManus 1991).

In an attempt to quantitatively capture these spatial relations, we have adapted a geostatistical modeling approach to the problem of forecasting gypsy moth defoliation. Geostatistics were originally developed in the earth sciences for describing and modeling petroleum and mineral reserves (Journel & Huijbregts 1978, Hohn 1988). Many

[1] West Virginia Geological and Economic Survey, P.O. Box 879, Morgantown, WV 26506–0879.

[2] USDA Forest Service, Northeastern Forest Experiment Station, 180 Canfield Street, Morgantown, WV 26505.

of these techniques have been adapted to ecological problems that involve modeling of spatial patterns (Robertson 1987, Rossi et al. 1992). Among these geostatistical techniques, "kriging" has been recognized as a useful method for modeling two-dimensional patterns (Kemp et al. 1989, Liebhold et al. 1991). The objective of our study was to adapt a variant of this method, called three-dimensional kriging, for modeling the spatial dynamics of gypsy moth outbreaks. Historical defoliation data from Massachusetts were used to parameterize a model that is used to ex trapolate defoliation maps into the future. This is a novel approach and may provide a useful way of increasing our ability to predict insect outbreaks.

Materials and Methods

Data. The Massachusetts Department of Environmental Management monitors gypsy moth defoliation annually in all parts of the state using aerial sketch maps. Maps are sketched during a series of low-level reconnaissance flights in late July when defoliation is at its peak. Thirty percent (30%) defoliation is considered the lower threshold for detection from the air. In situations where there is doubt as to the cause of the defoliation, ground checks for the presence of gypsy moth life stages are made. Initially the aerial sketch maps are overlaid on standard U.S. Geological Survey (1:24,000) topographical maps. Subsequently, a composite mosaic map is generated for the entire state at 1:760,000 scale. Mapping processes may vary from region to region and year to year in these sketch maps, possibily resulting in systematic and nonsystematic data errors (Talerico 1981, Chrisman 1987). The likely presence of these errors dictated a coarse spatial resolution in the digital representation of these maps (rasters 2 by 2 km).

A geographic information system (GIS), IDRISI, was used to assemble and collate gypsy moth defoliation data. (Eastman 1989). IDRISI is a raster-based (grid cell) GIS for capturing, storing, analyzing, and displaying geographical data, and is designed for research applications. A base map of Massachusetts county boundaries was used to define the study area. This map was generated from latitude and longitude coordinates (obtained from the SAS/GRAPH system) (SAS Institute 1987) and these coordinates were projected using the Azmuthal Equal-Distant Projection (Snyder 1987). This projection conserves true distance linearly from a designated point (Boston, MA). A grid cell size of 2 by 2 km was selected as standard for all map layers in the GIS. Each map layer comprised 198 by 93 cells.

To create a uniform set of geographically referenced defoliation data, the composite defoliation maps for the period 1960 to 1989 were first transferred to mylar stable-base sheets. At least four georeference points, on clearly recognizable intersections of county boundaries, were accurately located. The prepared maps were then scanned using a digital scanner set at 150 dots per inch resolution. Binary TIFF files from the scanner were converted to ASCII IDRISI image format and saved as IDRISI images or map layers. The transformation of each map layer to a common base map resolution and projection was achieved through a "rubber-sheeting" procedure. In transforming maps of various scales and projections, IDRISI resamples each scanned defoliation image to match the location of the four georeference points on the base map (Eastman 1987).

The compilation of the defoliation map layers from 1960 to 1990 resulted in a three-dimensional matrix (198 by 93 by 30) of binary (0, 1) data. Because the data were coded as either 0 or 1, depending on whether it exceeded the defoliation threshold (30%), the variable is considered an "indicator" variable. Several geostatistical procedures are available for quantifying and modeling spatial dependence in indicator values (Isaaks & Srivastava 1989, Kemp et al. 1989, Liebhold et al. 1991).

Measurement of Spatiotemporal Dependence. The variogram is commonly used in geostatistics to observe and model spatial dependence. Although it can be computed for irregularly distributed data in space, the easiest case is where points of observation are distributed on a regular grid, as is the case for the defoliation data analyzed above. If we define h to be the distance between two grid nodes or cells, then adjacent cells along rows or columns are separated by $h = 1$, alternate cells along rows or columns are separated by a distance of $h = 2$, and so forth. Adjacent cells along the diagonal are obviously separated by multiples of 1.414. For a given value of h, we can calculate the variogram statistic:

$$\gamma(h) = \frac{1}{2n_h} \sum_{k=1}^{n_h} [i(x_k) - i(x_k + h)]^2 \qquad (1)$$

where $i(x_k)$ is a value of the indicator variable (calculations are identical for the semivariance of a continuous variable) at location x_k, $i(x_k + h)$ is the value (in this case the value is the binary defoliation indicator variable) at a location h units from x_k, and n_h is the number of pairs used in calculating $\gamma(h)$ for a given value of h.

The statistic $\gamma(h)$ can be calculated for several values of h and plotted on the vertical axis versus h on the horizontal axis. The older literature refers to this graph as the "semivariogram" (Journel & Huijbregts 1978), but recent literature refers to both $\gamma(h)$ and the graph as the "variogram" (Isaaks & Srivastava 1989) and we use this term hereafter. In the presence of spatial dependence,

the number of pairs having $z(x_k) = z(x_k + 1)$ should be relatively large (i.e., adjacent cells both have values equal to 0 or 1). With increasing h, the chance of $z(x_k)$ and $z(x_k + h)$ having dissimilar values also increases, so the variogram increases. At a value of h called the range, spatial dependence disappears and the variogram levels off to a value called the sill. Under ideal conditions of stationarity and when the study area is large relative to the range, the sample variance equals the sill. Spatial dependence can be isotropic (the same in all directions) or anisotropic. Anisotropies are detected by partitioning pairs of cells by both distance, h, and direction and graphing a variogram for each direction.

Use of the variogram in subsequent estimation by kriging requires fitting a variogram model. We used the exponential model:

$$\gamma(h) = C(1 - e^{-h/a}) \quad (2)$$

where a and C are constants. The exponential model approaches C, the sill asymptotically, but to all appearances, reaches C at $h = 3a$, the "range." The complete variogram model can have the form:

$$\gamma(h) = \gamma_1(h) + \gamma_2(h) + \ldots \gamma_n(h) \quad (3)$$

where each $\gamma_i(h)$ is a component variogram model. These additive models are termed "nested models" (Isaaks & Srivastava 1989).

Variograms were calculated for a number of directions in space: east (0°), northeast to southwest (45°), north (90°), and northwest to southeast (135°), by partitioning pairs $i(x_k)$, $i(x_k + h)$ among four angle classes, each 45° wide, and 20 distance classes, each 1 raster unit (2 km) wide. We also computed a variogram along the time axis of the data using 20 distance classes, each one raster unit (1 yr) wide. Variogram models were fit by eye using procedures described by Hohn (1988, chapter 2).

Estimation. Linear estimation or "kriging" is a geostatistical procedure for estimating a value at a particular location as a weighted average of observed values at nearby locations (Journel & Huijbregts 1978, Hohn 1988, Isaaks & Srivastava 1989):

$$z^*(x_k) = \sum_{i=1}^{n} \lambda_i z(x_i) \quad (4)$$

where $z(x_i)$ is an observed value of the variable being estimated, λ_i is a corresponding weight, and $z^*(x_k)$ is the estimated value at a particular location x_k. Nearby locations generally have greater weights than points farther away, reflecting the underlying spatial structure of the data. Weights are calculated such that two criteria are satisfied: (1) the estimate is unbiased; (2) estimation variance is minimized.

The first criterion is satisfied by requiring the weights to sum to one. Estimation variance is computed from:

$$\sigma^2 = \overline{C}(V,V) - 2\sum_i \lambda_i \overline{C}(V,v_i) + \sum_i \sum_j \lambda_i \lambda_j \overline{C}(v_i,v_j) \quad (5)$$

where $\overline{C}(A,B)$ is the covariance between the regionalized variable at locations A and B; = sample variance $-$ $\gamma(A,B)$; V is the location of estimate; and v_i, v_j are locations of observed values.

The variogram value $\gamma(A,B)$ is obtained by computing the distance between locations A and B and using this h to calculate $\gamma(h)$ from the variogram model. $\overline{C}(V,V)$ is simply the covariance between a point and itself, which is the sample variance.

Estimation variance is minimized by solving the following system of equations:

$$\sum_{j=1}^{n} \lambda_j \overline{C}(v_i,v_j) - \mu = \overline{C}(v_i,V) \text{ for } i = 1,n \quad (6)$$

where μ is a Lagrange parameter,

$$\sum_{j=1} \lambda_j = 1. \quad (7)$$

As stated earlier, defoliation status is a binary indicator variable; the value was coded as 0 if it was less than the 30% threshold level and 1 if it was greater than the threshold. Consequently, kriged estimates of this variable were calculated as probabilities of exceeding the defoliation threshold. We write the defoliation probability at each cell (position in space and time is identified as x_k) in the 198 by 93 by 30 grid as $P(x_k)$; note that location x has two spatial components and a time component. Following from equation 4 the kriged estimate for $P^*(x_k)$ is a linear combination of the n observed values of $i(x_k)$ in spatial and temporal proximity to location x_k; i.e.,

$$P^*(x_k) = F^*(x_k)\left[1 - \sum_{j=1}^{n} w_j\right] + \sum_{j=1}^{n} w_j i(x_j) \quad (8)$$

in which $P^*(x_k)$ is an estimate of $P(x_k)$ and $F^*(x_k)$ is an estimate of the expected frequency that $i(x) = 1$.

The weights, w_j, were computed by means of a system of n equations:

$$\sum_{m=1}^{n} w_m \rho(x_m - x_1) = \rho(x_1 - x_k)$$

$$\sum_{m=1}^{n} w_m \rho(x_m - x_2) = \rho(x_2 - x_k)$$

$$\bullet$$

$$\bullet$$

$$\bullet$$

$$\sum_{m=1}^{n} w_m \rho(x_m - x_n) = \rho(x_n - x_k) \quad (9)$$

where ρ is the autocorrelation statistic:

$$\rho(a - b) = \rho(h) = 1 - \gamma(h) / \sum_{v=1}^{v} (C_v) \quad (10)$$

and $C_1, C_2 \ldots C_v$ are constants in the variogram model and h is the distance between locations a and b. The system of kriging equations is written in matrix form:

$$B \cdot W = D \quad (11)$$

where B, W, and D are the covariance, weight, and distance matrices, respectively; solving for the weights yields:

$$W = D \cdot B^{-1} \quad (12)$$

The geostatistical literature calls the estimation method used here "simple kriging" (Journel & Huijbregts 1978). It differs from the more commonly used procedure, "ordinary kriging," in that it requires a prior estimate of frequency, $F(x_k)$, for each candidate grid cell. In this study, this term represents an a priori expectation of the frequency of defoliation. A number of options exist for calculating $F^*(x_k)$. One approach is to predict $F^*(x_k)$ from variables that are associated with each grid cell. Examples of such variables include characteristics of the biological or physiographic landscape (Liebhold et al. 1993b), or the frequency could be calculated from census counts (e.g., egg mass counts [Liebhold et al. 1993a, Williams et al. 1991]). A second approach was used in this study: frequencies were calculated as averages from historical defoliation data. The total number of years of defoliation was divided by the total number of years (30) for each of the 6,075 grid cells falling within the state of Massachusetts. The resulting map (Fig. 1) shows clearly that some areas tend to be defoliated more often than others, reflecting the association of gypsy moth defoliation with specific forest types and physiographic features (Liebhold & Elkinton 1989, Liebhold et al. 1993b).

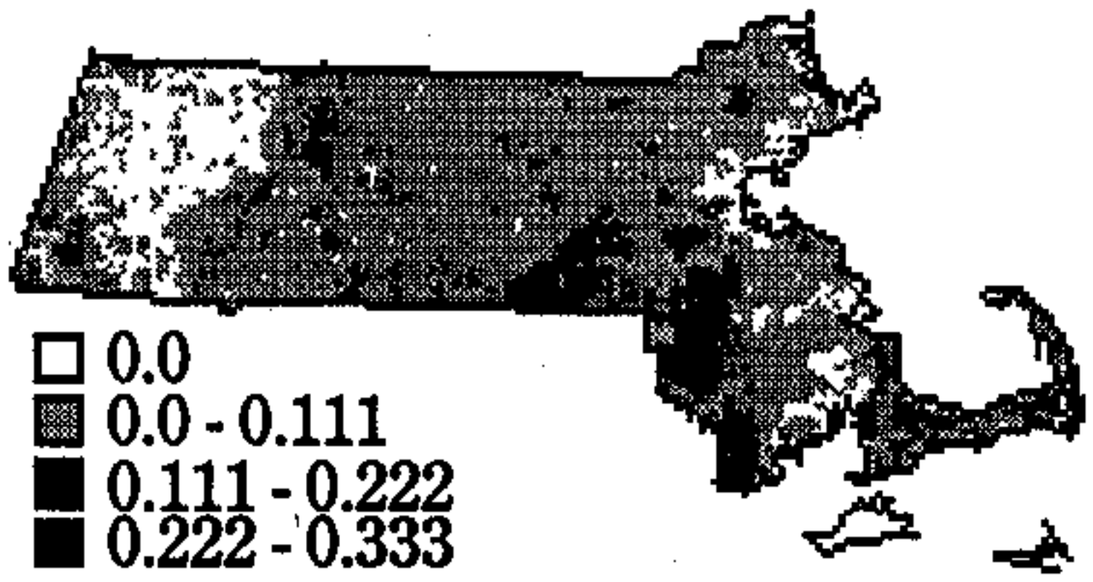

Fig. 1. Mapped defoliation frequencies for each 2 by 2 km raster in Massachusetts during 30 yr from 1961 to 1990.

Kriging methods have several desirable features regarding the weights w_j. In general, points closest to x_k have the largest corresponding weights. Variogram models can be anisotropic; that is, component variograms are damped in certain directions, or ranges vary with orientation (Isaaks & Srivastava 1989, Rossi et al. 1992). Because the kriging system of equations depends upon variograms fitted to observed data, weights are greatest for directions of least variation. Hence, kriging captures consistent directional trends in variability (see discussion by Hohn, 1988, 107).

A single variogram model was fit in all three dimensions (N–S, E–W, and time), with different ranges specified for space and time. Each grid cell was weighted both by its spatial and temporal distances from the point being estimated. By modeling the anisotropy, we were able to account for the arbitrary equivilance of units in spatial and temporal dimensions (i.e., 2 km = 1 yr).

Results and Discussion

Observed variograms (Fig. 2A) in the spatial domain exhibited nearly the same shape and could be fitted with a single, isotropic model; we used a nested exponential model:

$$\gamma(h) = 0.021(1 - e^{-h/0.7}) + 0.050(1 - e^{-h/40}) \quad (13)$$

The range of the first exponential term (0.7) was less than the distance between two adjacent grid cells, indicating spatial heterogeneity of defoliation at short distances. The magnitude of small-scale variability in defoliation was not large however; the ratio of the sill for this first term (0.021) to the total of the variogram (0.021 + 0.050) was only 0.30.

The variogram for the time domain (Fig. 2B) has a range of ≈5 yr (3 × 1.7 years), reaches a sill, then declines briefly. This "hole" in the variogram from lag distances of 9 through 15 yr results from the episodic nature of gypsy moth outbreaks; defoliation in an area is usually low to

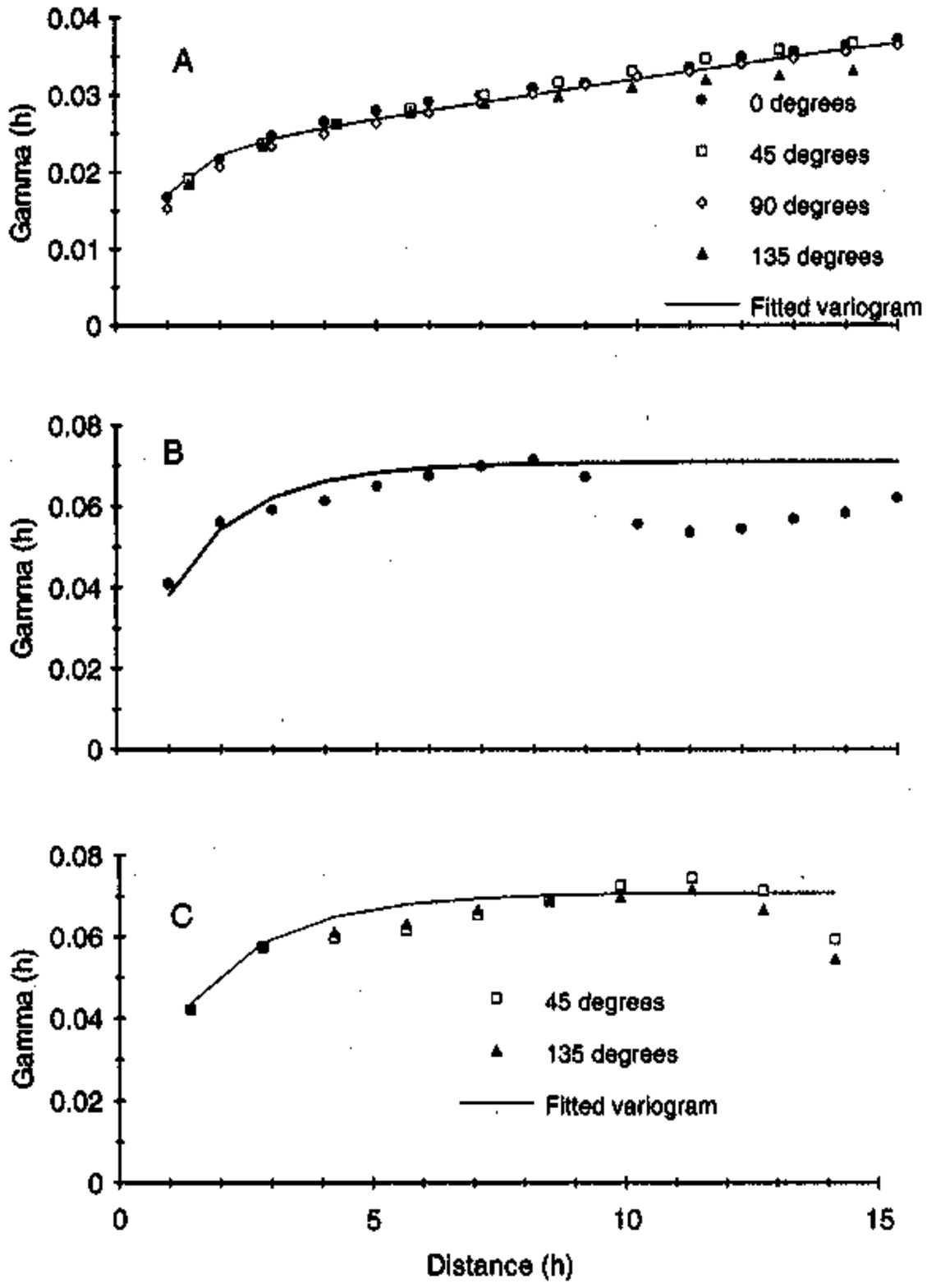

Fig. 2. Sample indicator variograms calculated in various directions from 1960–1990 defoliation data. Units on horizontal axes are numbers of cells (2 km by 2 km by 1 year). Dotted lines are the variogram model defined in equation 16. (A) The spatial domain in each of four directions: east–west (0°), northeast–southwest (45°), north–south (90°), northwest–southeast(135°). (B) The time domain. (C) The space–time domain (this is the 45° angle in the time by east–west plane).

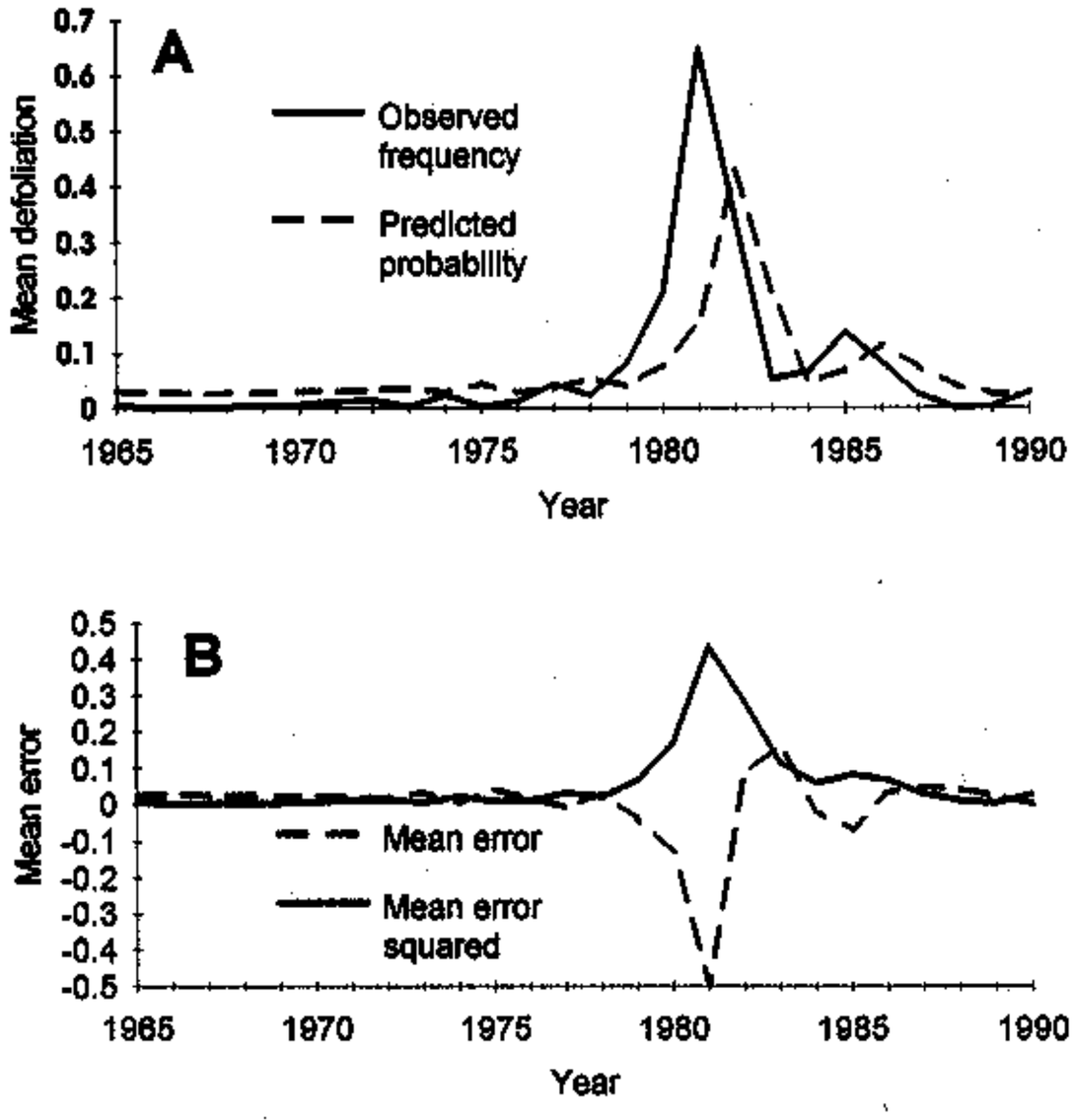

Fig. 3. Yearly observed and predicted defoliation from 1965 to 1990. (A) Observed frequency of defoliation and mean probability of defoliation in Massachusetts. (B) Yearly error statistics summarizing the difference between observed defoliation and predicted defoliation probabilities.

zero, and outbreaks persisted for several years (Fig. 3A). The variogram model for time was identical to that for space except for the shorter range of the second exponential term:

$$\gamma(h) = 0.021(1 - e^{-h/0.7}) + 0.050(1 - e^{-h/1.7}) \quad (14)$$

Together, the two models comprise a single, anisotropic model in both space and time:

$$\gamma(h) = 0.021(1 - e^{-h/0.7}) + 0.050(1 - e^{-h/r}) \quad (15)$$

where

$$r = \frac{r_s r_t}{\sqrt{r_s^2 \sin^2\phi + r_t^2 \cos^2\phi}} \quad (16)$$

and r_s is the range of spatial variogram (40.0), r_t is the range of temporal variogram (1.7), and ϕ is the azimuth of the vector separating two locations relative to the spatial plane.

As a check, r for the variogram in the spatial plane is calculated from equation 16:

$$r = \frac{r_s r_t}{\sqrt{r_s^2 \sin^2\phi + r_t^2 \cos^2\phi}} =$$

$$\frac{r_s r_t}{\sqrt{\phi + r_t^2}} = r_s \quad (17)$$

Similarly, r for the variogram in the time domain is equal to r_t. The expression for r in terms of r_s and r_t (equation 16) follows from the definition of a geometric anisotropy (Journal & Huijbregts 1978). Combined space–time variograms (e.g., 45° in the space–time plane) need not be fitted; the space–time model (calculated from equation 15; Fig. 1C) shows an excellent fit to observed variograms in two directions.

The use of an anisotropic variogram model (equation 15) for both spatial and temporal directions avoids the assumption of any innate equivalence between spatial and temporal measurement units. In addition, separate spatial and temporal variogram models can lead to nonunique solutions of the kriging systems of equations (Myers & Journel 1990, Rouhani & Myers 1990)

A kriged estimate for each location x_k in a given year was computed from observed defoliation in the two previous years and the 49 locations within a 7 by 7 grid centered on x_k. This configuration of cells, or "search radius," was

selected because the spatial variogram range (equation 13) was larger than the temporal range (equation 14), and locations approaching and beyond the range had near-zero weights and made little contribution to the final estimates. In this manner, defoliation probability maps were estimated from 1963 to 1990 (Fig. 4). Estimates could not be reliably derived for 1960–1962 because of inadequate defoliation data in preceding years.

The sequence of estimates graphed by year (Fig. 4) show that kriging has modified the cumulative defoliation frequencies shown in Fig. 1 to reflect more accurately the particular spatial patterns in defoliation during previous years. In addition, the maps of probabilities often have about the same appearance as the observed maps in the sense that areas of high defoliation probability typically corresponded to areas of observed defoliation (Fig. 4).

The kriging procedure performed best, in terms of delineating areas of predicted defoliation, during the peak years of defoliation (Fig. 4). The predicted spatial distribution of defoliation corresponded more poorly with the observed distribution during the initial years of gypsy moth outbreak such as 1973 and the lull in 1983. During the peak year 1981, defoliation was extensive through most of Massachusetts. The kriged probabilities for that year show very high values over most of the area, a correct prediction from the numerous, scattered sites of defoliation in the previous year. In contrast, the second main outbreak during 1984–1987 was much more compact in area; this was reflected in kriged estimates.

For each year, histograms showing the frequency distributions of cell defoliation probabilities were calculated for defoliated and nondefoliated cells; Fig. 5 shows histograms for 3 representative yr. These histograms showed that defoliation probabilities were generally higher for defoliated cells than they were for undefoliated cells. For each year, we computed the mean error:

$$\frac{\sum_{k=1}^{n} P^*(x_k) - i(x_k)}{n}$$

and the mean squared error:

$$\frac{\sum_{k=1}^{n} [P^*(x_k) - i(x_k)]^2}{n}.$$

These statistics, graphed by year, show the largest model error for years having moderate to dense defoliation levels (Fig. 3B). The peaks in the graph of the squared error correspond to the year of maximum outbreak, 1981. In general, the mean predictions of defoliation tended to lag 1 yr behind the observed defoliation frequency (Fig. 3A). Kriged estimates of defoliation in any year t tend to be very similar in both magnitude and spatial distribution to defoliation patterns in year $t - 1$ (Fig. 4). This is why, in years preceding the large 1981 outbreak when populations were rising, predicted probabilities were too low, but in years following the 1981 peak defoliation, the predicted probabilities were too high (Fig. 2B and 3A).

The modeling approach presented here is completely empirical; as such it is based completely upon the persistence and spread of defoliation through time. Although specific biological processes are not explicitly modeled, the persistence and spread of defoliation reflects the emergent properties of a multitude of ecological factors. The statistical persistence of defoliation reflects a certain level of stability in high-density populations that causes outbreaks to persist for several years (Liebhold 1992). Liebhold & McManus (1991) described the apparent spread of defoliation and presented several mechanisms that might cause it. They concluded it was unlikely that the observed spread of outbreaks was caused by the dispersal of gypsy moths from high to low density areas. Instead, they concluded that populations may rise synchronously over large areas, and the apparent spread of defoliation actually was caused by the spatial distribution of susceptibility.

The space–time variogram model presented here is specific to the scale at which we measured space and time; our data were measured using cells of 2 km by 2 km by 1 yr. The dynamic patterns exhibited by gypsy moth populations can be quite different when populations are aggregated at different spatial scales (Liebhold 1992).

The three-dimensional kriging procedure described here is probably not suitable for operational use; even though the spatial distribution of outbreak predictions often coincided well with observed defoliation patterns, the magnitude of the region-wide outbreak generally lagged behind actual values. Nevertheless, we feel that this is a novel approach to forecasting insect outbreaks and that these types of landscape-level models, with modification, may ultimately outperform traditional forecasting systems. Incorporation of yearly insect census data (e.g., point estimates of overwintering egg mass densities) into these time-space models may be one type of modification of these models that would result in forecasts that more closely track actual year-to-year population levels.

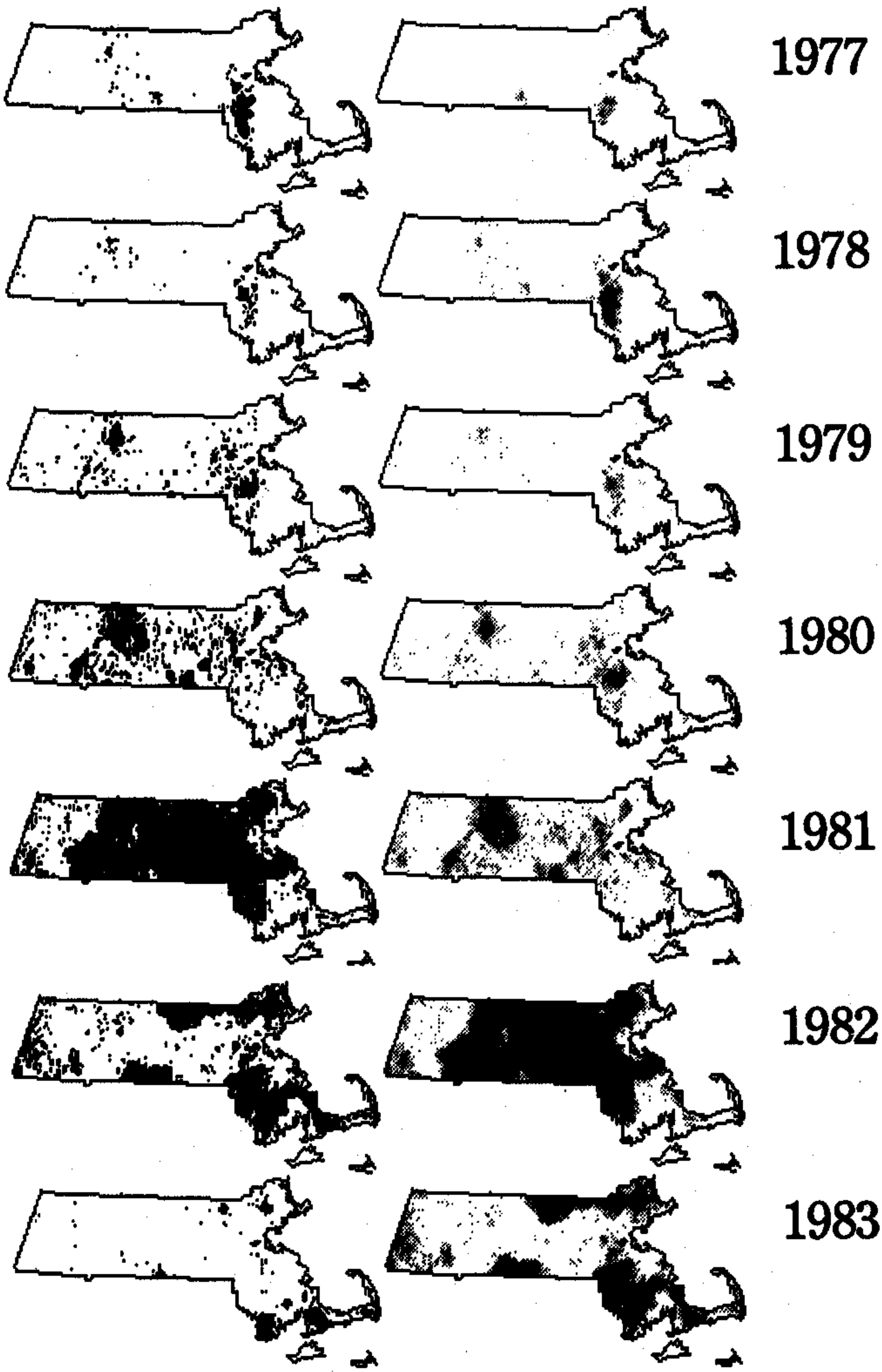

Fig. 4. Predicted defoliation probabilities (using time–space kriging model) and observed defoliation maps for Massachusetts, 1977–1990.

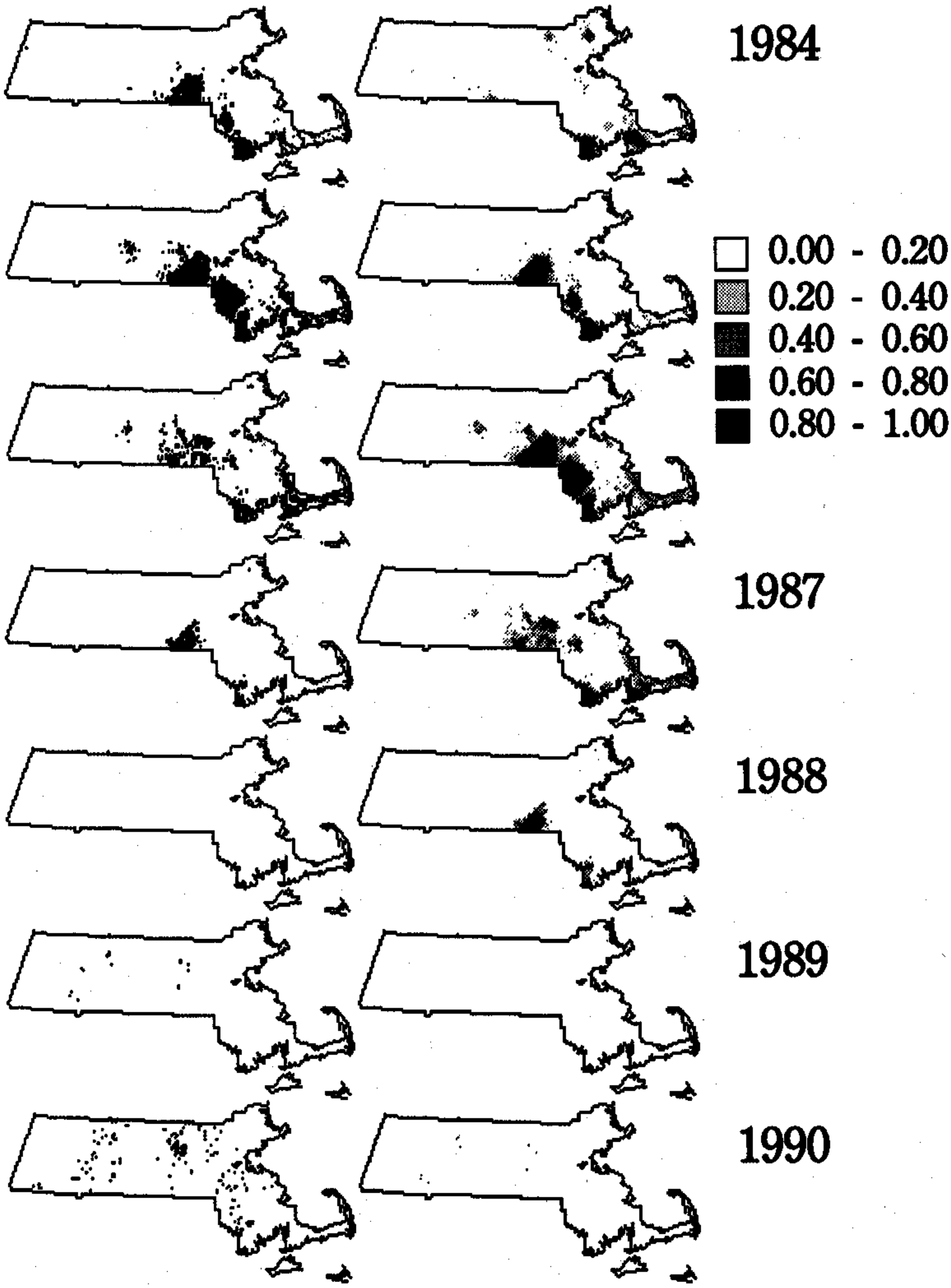

Fig. 4. Continued

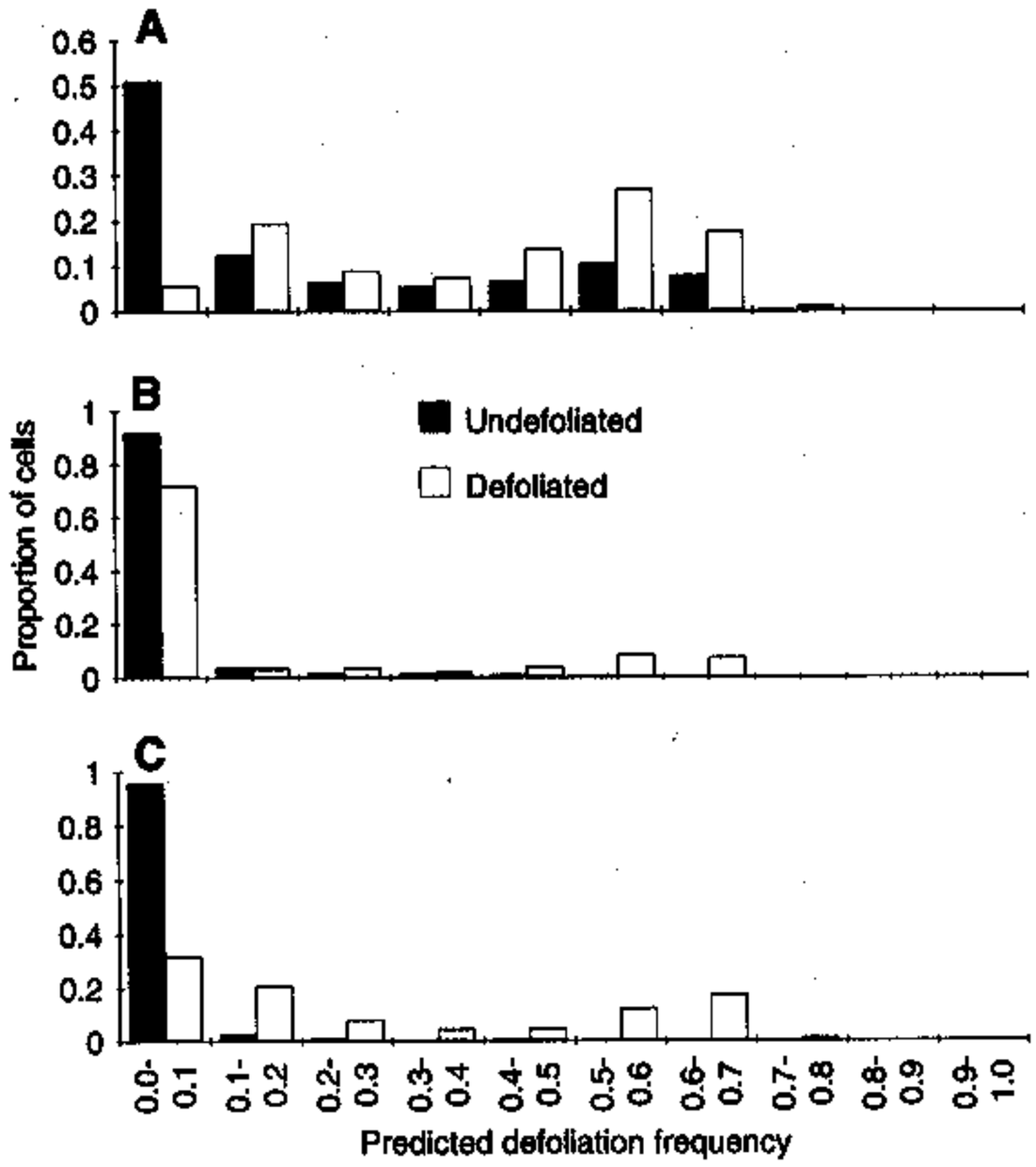

Fig. 5. Frequency distributions of predicted probabilities of defoliation for defoliated and nondefoliated cells. (A) 1983. (B) 1984. (C) 1985.

Acknowledgments

We thank Eugene Luzader (USDA Forest Service), who helped in many aspects of this research, and the Massachusetts Department of Environmental Management for providing defoliation data. We are grateful to Rick Rossi (Isaaks & Co.) and Dennis Schotzko (University of Idaho) for reviewing an earlier draft of this manuscript. This research was funded in part by the USDA Forest Service Gypsy Moth Research and Development program and by grants 89-37250-4533 and 91-37302-6278 from the USDA–CSRS Competitive Grants Program.

References Cited

Campbell, R. W. 1967. The analysis of numerical change in gypsy moth populations. For. Sci. Monogr. 15.

Campbell, R. W. & J. P. Standaert. 1974. Forecasting defoliation by the gypsy moth in oak stands. USDA For. Serv Res. Note NE-193.

Chrisman, N. R. 1987. The accuracy of map overlays: a reassessment. Landscape and Urban Plann. 14: 427–439.

Clark, I. 1979. Practical geostatistics. Applied Science, London.

Eastman, J. R. 1989. IDRISI: a grid-based geographical analysis system. Clark University Press, Worcester, MA.

Gansner, D. A. & O. W. Herrick. 1982. Predicting the rate of change in timber value for forest stands infested with gypsy moth. USDA For. Serv. Res. Note. NE-311.

Hohn, M. E. 1988. Geostatistics and petroleum geology. Van Nostrand Reinhold, New York.

Isaaks, E. H. & R. M. Srivastava. 1989. An introduction to applied geostatistics. Oxford University Press, New York.

Journel, A. G. & C. J Huijbregts. 1978. Mining geostatistics. Academic, London.

Kemp, W. P., T. M. Kalaris & W. F. Quimby. 1989. Rangeland grasshopper (Orthoptera: Acrididae) spatial variability: macroscale population assessment. J. Econ. Entomol. 82: 1270–1276.

Liebhold, A. M. 1992. Are North American gypsy moth poulations bimodal? Environ. Entomol. 21: 221–229.

Liebhold, A. M. & J. S. Elkinton. 1989. Characterizing spatial patterns of gypsy moth regional defoliation. For. Sci. 35: 557–568.

Liebhold, A. M. & M. J. McManus. 1991. Does larval dispersal cause the spread of gypsy moth outbreaks? N. J. Appl. For. 8: 95–98.

Liebhold, A. M., X. Zhang, M. E. Hohn, J. S. Elkinton, M. Ticehurst, G. L. Benzon & R. W. Campbell. 1991. Geostatistical analysis of gypsy moth (Lepidoptera: Lymantriidae) egg mass populations. Environ. Entomol. 20: 1407–1417.

Liebhold, A. M., E. Simons, A. Sior & J. Unger. 1993a. Predicting gypsy moth defoliation from field measurements. Environ. Entomol. 22: 26–32.

Liebhold, A. M., G. A. Elmes, J. A. Halverson & J. Quimby. 1993b. Landscape characterization of forest susceptibility to gypsy moth defoliation. For. Sci. (in press).

Myers, D. E. & A. Journel. 1990. Variograms with zonal anisotropies and noninvertible kriging systems. Math. Geol. 22: 779–785.

Montgomery, M. E. 1990. Role of site and insect variables in forecasting defoliation by the gypsy moth, pp. 73–84. *In* A. D. Watt et al. [eds.], Population dynamics of forest insects. Intercept, Andover, UK.

Price, P. W., N. Cobb, T. P. Craig, G. W. Fernandes, J. K. Itami, S. Mopper & R. W. Preszler. 1990. Insect herbivore population dynamics on trees and shrubs: new approaches relevant to latent and eruptive species and life table development, pp. 1–38. *In* E. A. Bernays [ed.], Insect–Plant Interaction, vol. 2. CRC, Boca Raton, FL.

Ravlin, F. W., R. G. Bellinger & E. A. Roberts. 1987. Gypsy moth management programs in the United States: status, evaluation and recommendations. Bull. Entomol. Soc. Am. 33: 90–98.

Robertson, G. P. 1987. Geostatistics in ecology: interpolating with known variance. Ecology 68: 744–748.

Rossi, R. E., D. J. Mulla, A. G. Journel & E. H. Franz. 1992. Geostatistical tools for modeling and interpreting ecological spatial dependence. Ecological Monogr. 62: 277–314.

Rouhani, S. & D. E. Myers. 1990. Problems in space–time kriging of geohydrological data. Math. Geol. 22: 611–623.

SAS Institute. 1987. SAS/GRAPH guide for personal computers, version 6 Edition. SAS Institute, Cary, NC.

Snyder, J. P. 1987. Map projections\a working manual. U.S. Geol. Surv. Prof. Pap. 1395.

Sokal, R. R. & F. J. Rohlf. 1981. Biometry. Freeman, San Francisco.

Talerico, R. L. 1981. Defoliation as an indirect means of population assessment, pp. 38–49. *In* C. C. Doane & M. L. McManus [eds.], The gypsy moth: research toward integrated pest management. USDA Tech. Bull. 1584.

Williams, D. W., R. W. Fuester, W. W. Metterhouse, R. J. Balaam, R. H. Bullock & R. J. Chianese. 1991. Oak defoliation and population density relationships for the gypsy moth. J. Econ. Entomol. 84: 1508–1514.

Received for publication 25 June 1992; accepted 23 April 1993.